



# A STUDY OF THE EFFECT OF THE MORPHOLOGY ON THE PHOTOCATALYTIC ACTIVITY OF WO<sub>3</sub>

Dávidné Nagy<sup>[a]</sup>, Tamás Firkala<sup>[b]</sup>, Xianfeng Fan<sup>[a]</sup> and Imre Miklós Szilágyi<sup>[b,c]\*</sup>

**Keywords:** WO<sub>3</sub>, hexagonal, monoclinic, nanoparticle, nanowire, photocatalysis.

The photocatalytic activity of hexagonal (h-) WO<sub>3</sub> nanoparticles (NPs) and nanowires (NWs) was investigated and compared with the performance of monoclinic (m-) WO<sub>3</sub> nanoparticles in the aqueous photo-bleaching reaction of methyl orange (MO) under UV irradiation. It has been known that the m-WO<sub>3</sub> is better photocatalyst than the h-WO<sub>3</sub>, but due to the advantageous morphology we investigated whether the h-WO<sub>3</sub> NWs can reach the photo-efficiency of the m-WO<sub>3</sub> NPs. The h-WO<sub>3</sub> was successfully synthesized in NW and NP morphology using a microwave (MW) assisted hydrothermal procedure starting from Na<sub>2</sub>WO<sub>4</sub> and thermal annealing of hexagonal ammonium tungsten bronze (HATB), (NH<sub>4</sub>)<sub>0.33-x</sub>WO<sub>3</sub>, respectively. We found that the h-WO<sub>3</sub> NWs exhibited almost three times higher photoactivity than the h-WO<sub>3</sub> NPs. The improved performance of the NWs can be attributed to the enlarged surface area and the good charge carrier ability of the nanowire morphology. The catalytic tests also confirmed that the morphological effect could lead to as high photoactivity in the case of h-WO<sub>3</sub> NWs as exhibited by the m-WO<sub>3</sub> NPs.

\* Corresponding Authors

FAX: +36-1-4633408

Email: imre.szilagyi@mail.bme.hu

- [a] University of Edinburgh, The King's Buildings, Mayfield Road, Edinburgh, EH9 3JL, UK  
 [b] Budapest University of Technology and Economics, Department of Inorganic and Analytical Chemistry, Szent Gellért tér 4., Budapest, H-1111, Hungary  
 [c] MTA-BME Research Group of Technical Analytical Chemistry, Szent Gellért tér 4., Budapest, H-1111, Hungary

## Introduction

In the last few decades much attention has been attracted by alternative energy resources including renewable and nuclear fusion energy due to the limitation of availability of fossil fuel on the earth. Exploiting solar light for future energy is one of the highly studied possibilities as it can provide environmental friendly and renewable source of energy. Photocatalysts are able to convert solar energy into chemical energy which can be used for numerous purposes like generation of hydrogen fuel through water splitting; purification of different aqueous media; green synthesis of various chemicals.<sup>1</sup>

TiO<sub>2</sub> was historically the first photocatalyst and still remained one of the most efficient photocatalysts under UV light. However, the large band gap energy of TiO<sub>2</sub> makes its application in solar photocatalysis insufficient. An option to develop solar sensitive photocatalyst is to couple TiO<sub>2</sub> with other semiconductors, which absorb in the Vis range. As a beneficial consequence of making composites with TiO<sub>2</sub>, delayed recombination of the photo-generated charges can be provided. The electrons and holes can be effectively separated in the different semiconductor layers resulting in higher photo-efficiency. Narrow band gap semiconductors like WO<sub>3</sub>, V<sub>2</sub>O<sub>5</sub>, Bi<sub>2</sub>O<sub>3</sub> are usually considered to form a heterojunction with TiO<sub>2</sub>.<sup>2-4</sup>

WO<sub>3</sub> attracted much attention recently, owing to its broad application prospective and advantageous chemical and electrical properties.<sup>4,5</sup> WO<sub>3</sub> is a good candidate for the fabrication of solar response photocatalyst with TiO<sub>2</sub> as it has absorption in the Vis range.<sup>6</sup> The photocatalytic activity depends on many factors, and numerous attempts were made in order to control the size distribution and the dimensionality of the nanocatalysts, because these are considered as key parameters in affecting their photocatalytic performance.<sup>7-10</sup> Various morphologies have already been achieved including nanotrees, nanorods, nanospheres etc.<sup>9,11,12</sup> Unexpectedly, it was recently reported that despite their high specific surface area in some cases certain WO<sub>3</sub> particles showed lower photo-efficiency.<sup>13</sup> The peculiar finding was accounted for the facilitated charge recombination which surpassed the positive effect of the enlarged surface area. It is also known that the crystalline phase and the composition of WO<sub>3</sub> play an important role in the photo-efficiency. It was revealed that usually m-WO<sub>3</sub> possesses better photocatalytic ability than h-WO<sub>3</sub>.<sup>14</sup>

Considering these factors, in this study we aimed to investigate the overall effect of the morphology on the photocatalytic performance of different polymorphs of WO<sub>3</sub>, with the pronounced future objective to fabricate solar active nanocomposites by coupling WO<sub>3</sub> polymorphs with TiO<sub>2</sub>.

## Experimental

H-WO<sub>3</sub> nanoparticles were prepared by thermal annealing of hexagonal ammonium tungsten bronze (HATB), (NH<sub>4</sub>)<sub>0.33-x</sub>WO<sub>3</sub> at 470 °C in air.<sup>15</sup> H-WO<sub>3</sub> NWs were obtained in a microwave (MW) assisted hydrothermal synthesis at 160 °C.<sup>5</sup>

The reaction mixture was prepared from sodium tungstate dihydrate (Na<sub>2</sub>WO<sub>4</sub>·2H<sub>2</sub>O), ammonium sulphate ((NH<sub>4</sub>)<sub>2</sub>SO<sub>4</sub>), HCl and distilled water followed by the MW process in a Synthos 3000 Anton Paar reactor. After the synthesis the nanocrystals were centrifuged, washed with water and ethanol and finally dried at 80 °C for 24 h. For the preparation of the m-WO<sub>3</sub> NPs, (NH<sub>4</sub>)<sub>0.33-x</sub>WO<sub>3</sub> was annealed at 600 °C in air.<sup>15</sup>

The morphology of the as-prepared catalysts was investigated by TEM, and the images were collected by a FEI Morgagni 268D instrument. The determination of the crystalline phase of the WO<sub>3</sub> photocatalysts was confirmed both XRD and Raman spectroscopy. The XRD measurements were carried out by a PANalytical X'pert Pro MPD X-ray diffractometer using Cu K $\alpha$  radiation. Whereas the Raman spectra were obtained by a Jobin-Yvon Labram type Raman spectrometer coupled with an Olympus BX-41 microscope. An Nd-YAG laser with a wavelength of 532 nm was applied as a light source in the Raman spectrometer. The specific surface area was determined by applying the BET model based on the absorption isotherm of nitrogen at 77 K using NOVA 2000E equipment (Quantachrome, USA).

The photocatalytic activity was measured in aqueous methyl orange (MO) (10 mg/350 ml) solution under UV irradiation. In a typical test 100 mg catalyst powder was suspended in the MO solution. The photo-reactor was a cylindrical glass reactor equipped with a Heraeus TQ 150 mercury immersion lamp. The solution was stirred and oxygen bubbling was provided. Room temperature was maintained by circulating cold water in the jacket of the photo-reactor. The concentration of MO was followed by a Jasco V-550 type UV-Vis spectrophotometer at 465 nm.

## Results and Discussion

The XRD analysis confirmed that microwave assisted hydrothermal synthesis and annealing of HATB at 470 °C in air lead to the formation of hexagonal phase WO<sub>3</sub> (33-1387) with no crystalline impurities present in the diffractogram. The thermal annealing process of HATB at 600 °C in air resulted in the formation of monoclinic phase WO<sub>3</sub> (43-1035) as confirmed by the XRD pattern.

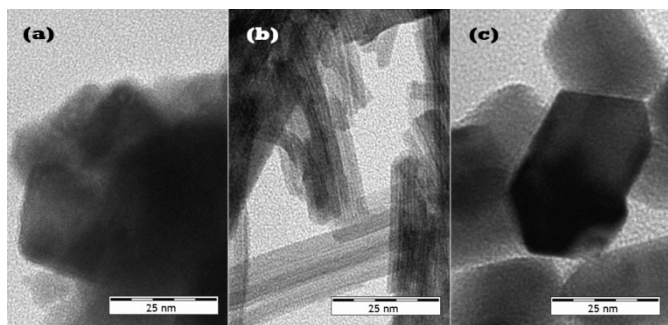


**Figure 1.** TEM images of (a) h-WO<sub>3</sub> NPs; (b) h-WO<sub>3</sub> NWs; (c) m-WO<sub>3</sub> NPs.

The morphology of the nanostructures was confirmed by TEM (Figure 1). The images revealed that the h-WO<sub>3</sub> NWs had diameters between 5 and 10 nm and were several

hundred nm long. The h-WO<sub>3</sub> NPs consisted of 50-70 nm particles, while the m-WO<sub>3</sub> NPs were made up by 60-90 nm particles.

The BET specific surface area of the h-WO<sub>3</sub> NP and NW was found to be 11 m<sup>2</sup>g<sup>-1</sup> and 101 m<sup>2</sup>g<sup>-1</sup>, respectively. The nanowire morphology resulted in one order of magnitude higher specific surface area, compared to that of the nanoparticle.<sup>14</sup>

The Raman spectra were in good agreement with the literature and with the XRD analysis and confirmed the hexagonal and monoclinic crystalline phase of the WO<sub>3</sub> nanostructures.<sup>14</sup>

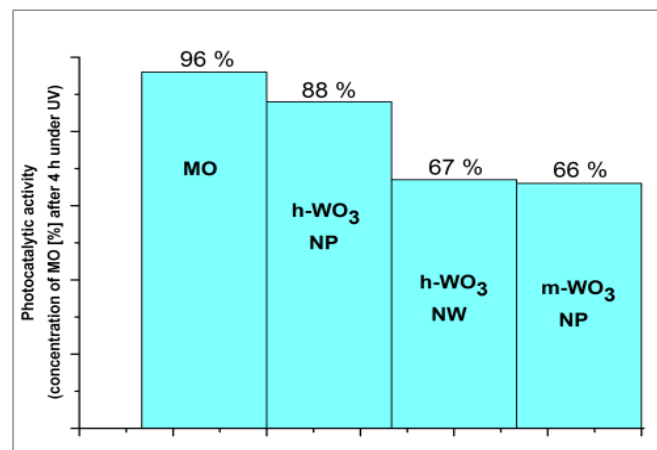


**Figure 2.** MO concentrations given in percentage after 4 hour UV irradiation in the photocatalytic test reaction.

In the photocatalytic test we found that the h-WO<sub>3</sub> NWs were almost three times more effective in the degradation of MO than h-WO<sub>3</sub> NPs (Figure 2). By the end of the 4 h UV irradiation, 12 % of the initial MO was decomposed by the h-WO<sub>3</sub> NPs, while the h-WO<sub>3</sub> NWs photo-bleached 33% of the original concentration of MO. The remarkable improvement in the photocatalytic activity could be attributed to the beneficial morphology of the h-WO<sub>3</sub> NWs. The findings also confirmed how important the precise control is over the morphology. The nanowire structure can provide better carrier transport to the separated charges and possess higher specific surface area leading to triple efficiency. The performance of h-WO<sub>3</sub> NWs was compared with the activity of m-WO<sub>3</sub> NPs as well. It was concluded that by the end of the photocatalytic test the h-WO<sub>3</sub> NWs were even more efficient (34 % MO decomposed) than the nanoparticles of the inherently better photocatalyst m-WO<sub>3</sub> (33 % MO decomposed). This finding revealed that the h-WO<sub>3</sub>, which attracted much interest due to its unique open-tunnel structure, can also achieve similarly high photon efficiency as m-WO<sub>3</sub>.

## Conclusions

In this study we successfully synthesized h-WO<sub>3</sub> both with NW and NP morphology along with m-WO<sub>3</sub> with NP nanostructure, either by a MW assisted hydrothermal synthesis route or by annealing (NH<sub>4</sub>)<sub>0.33-x</sub>WO<sub>3</sub>. The crystal phase of the nanostructures was confirmed by Raman spectroscopy while the microstructures were investigated by

TEM. The morphological effect on the photo-efficiency of the synthesized h- and m-WO<sub>3</sub> nanostructures was elucidated. The photoactivity of the h-WO<sub>3</sub> NWs was almost three times higher compared to that of the h-WO<sub>3</sub> NPs. The significant improvement in the photo-efficiency clearly indicated the positive effect of the high aspect ratio of the NWs, which could provide more enhanced carrier transport in the photocatalytic reaction than the NP nanostructure. We also examined the question whether the h-WO<sub>3</sub> NWs can exhibit as high photoactivity as the m-WO<sub>3</sub> NPs, which have been otherwise considered to be better photocatalysts. It was found that by the degradation test the h-WO<sub>3</sub> NWs surpassed even the performance of m-WO<sub>3</sub> NPs to a small extent.

## Acknowledgements

D. N. thanks to the University of Edinburgh for the Principle Career Development Scholarship. I. M. S. thanks for a János Bolyai Research Fellowship of the Hungarian Academy of Sciences. An OTKA-PD-109129 grant is gratefully acknowledged. The help of Dr. Eszter Drotár, Dr. Attila L. Tóth, Dr. Ágnes Szegedi (Research Centre for Natural Science, Hungarian Academy of Sciences) and Dr. Krisztina László (Department of Physical Chemistry and Materials Science, Budapest University of Technology and Economics) in parts of the experimental work is acknowledged.

## References

- <sup>1</sup>Mills, A., Le Hunte S., *J. Photochem. Photobio. A*, **1997**, *108*, 1.
- <sup>2</sup>Wojtyła, S., Baran, T., *Eur. Chem. Bull.*, **2015**, *4*, 260.
- <sup>3</sup>Wang, Y., Wang, Y., Zhang, J., Liu, L., Zhua, C., Liu, X., Su, Q., *Mater. Lett.*, **2012**, *75*, 95.

- <sup>4</sup>Szilágyi, I. M., Heikkilä, M., Pore, V., Kemell, M., Nikitin, T., Teucher, G., Firkala, T., Khriachtchev, L., Räsänen, M., Ritala, M., Leskelä, M., *Chem. Vapor Dep.*, **2013**, *19*, 149.
- <sup>5</sup>Arutanti, O; Ogi, T., Nandiyanto, A.B.D., Iskandar, F., Okuyama, K., *AIChE J.*, **2014**, *60*, 41.
- <sup>6</sup>Phuruangrat, A., Ham, D. J., Hong, S. J., Thongtem, S., Lee, J. S., *J. Mater. Chem.*, **2010**, *20*, 1683.
- <sup>7</sup>Xu, Z., Tabata, I., Hirogaki, K., Hisada, K., Wang, T., Wang, S., Hori, T., *Mater. Lett.*, **2011**, *65*, 1252.
- <sup>8</sup>Han, X; Han, X., Li, L., Wang, C., *New. J. Chem.*, **2012**, *36*, 2205.
- <sup>9</sup>Zhang, J., Wang, X. L., Xia, X. H., Gu, C. D., Tu, J. P., *Sol. Energ. Mater. Sol. Cell.*, **2011**, *95*, 2107.
- <sup>10</sup>Wang, X., Meng, X., Zhong, M., Wu, F., Li, J., *Appl. Surf. Sci.* **2013**, *282*, 826.
- <sup>11</sup>Van Tong, P., Hoa, N. D., Quang, V. V., Van Duy, N., Van Hieu, N., *Sens. Actuat. B*, **2013**, *183*, 372.
- <sup>12</sup>Li, J., Zhao, Q. L., Zhang, G. Y., Chen, J. Z., Zhong, L., Li, L., Huang, J., Ma, Z., *Solid State Sci.*, **2010**, *12*, 1393.
- <sup>13</sup>Amano, F., Ishinaga, E., Yamakata, A., *J. Phys. Chem. C*, **2013**, *117*, 22584.
- <sup>14</sup>Szilágyi, I. M., Fórizs, B., Rosseler, O., Szegedi, Á., Németh, P., Király, P., Tárkányi, G., Vajna, B., Varga-Josepovits, K., László, K., Tóth, A. L., Baranyai P., Leskelä, M., *J. Catal.* **2012**, *294*, 119.
- <sup>15</sup>Szilágyi, I. M., Madarász, J., Pokol, G., Király, P., Tárkányi, G., Saukko, S., Mizsei, J., Tóth, A. L., Szabó A., Varga-Josepovits, K., *Chem. Mater.*, **2008**, *20*, 4116.

Received: 13.02.2016.

Accepted: 29.02.2016.